Susceptibility of large populations of coupled oscillators

Hiroaki Daido

Department of Mathematical Sciences, Graduate School of Engineering, Osaka Prefecture University, Sakai 599-8531, Japan
(Received 24 November 2014; published 28 January 2015)

It is an important and interesting problem to elucidate how the degree of phase order in a large population of coupled oscillators responds to a synchronizing periodic force from the outside. Here this problem is studied analytically as well as numerically by introducing the concept of *susceptibility* for globally coupled phase oscillators with either nonrandom or random interactions. It is shown that the susceptibility diverges at the critical point in the nonrandom case with Widom's equality satisfied, while it exhibits a cusp in the most random case.

I. INTRODUCTION

Large populations of coupled oscillators play a crucial role in quite a few disciplines of science and technology, for example, physics, chemistry, biology, physiology (including the study of neural systems), and electronics [1–3]. The dynamics of such large-scale dynamical systems features the remarkable phenomenon of macroscopic entrainment or synchronization, which takes place when the coupling strength is strong enough to compensate for the desynchronizing effect due to the distribution of intrinsic frequencies. Some decades ago, it was pointed out that the onset of macroscopic synchronization is analogous to second-order phase transitions in thermodynamic systems, such as magnets and dielectrics [4]. This analogy to equilibrium critical phenomena has been quite helpful and led to the rapid development in the study of macroscopic synchronization, as we now actually see [2,3,5,6].

Phase transitions in equilibrium systems are characterized by the behavior of order parameters and quantities measuring their sensitivity to weak external perturbations. In the case of magnetic substances, a typical order parameter is the magnetization that quantifies the degree of orientational order of spins and the magnetic susceptibility specifies its response to an infinitesimal magnetic field applied from the outside. Their scaling behaviors near and at magnetic phase transitions play equally important roles in the area of critical phenomena [7]. In terms of coupled oscillators, the counterpart of the magnetization is Kuramoto's order parameter Z [2] and its generalized version introduced in Ref. [8] (see also Ref. [9]):

$$Z_k \equiv \frac{1}{N} \sum_{j=1}^{N} e^{ik\theta_j} \quad (k = \pm 1, \pm 2, \ldots), \quad (1)$$

where θ_j is the phase of the jth oscillator and $Z = Z_1$. These quantities are measures of phase order in large ensembles of coupled oscillators. Generally speaking, they will undergo some change when the system is subject to a weak periodic force, which is analogous to the magnetic field mentioned above. If a counterpart of the magnetic susceptibility is introduced in this context, then it will be one of variable tools to investigate the dynamics of oscillator populations, in particular, in the study of the synchronization transition. Practically, any knowledge of its universal behavior will be key information, for example, for the purpose of controlling oscillator assemblies using a weak cyclic signal.

The purpose of this work is to introduce the susceptibility as mentioned above and elucidate its behavior both analytically and numerically. For simplicity, in this paper, we confine ourselves to large populations of globally coupled phase oscillators with a frustration-free coupling proposed by the author a few decades ago [10]. This coupling is in general random, but includes the case of uniform coupling as a particular case, in which case the model becomes the Kuramoto model [11]. In what follows, the present work focuses on the susceptibility associated with the order parameter Z and shows that in the case of uniform coupling, it diverges at the critical point of macroscopic synchronization with the power of -1, while it exhibits a cusp under the most random coupling when the system enters a spurious glass phase [10] (see below). In the former coupling, it is also confirmed that the Widom equality holds, which is one of scaling law relations established for equilibrium cooperative phenomena [7].

The present paper includes four more sections: Section II is devoted to a description of the model and introduction of the concept of susceptibility. Then, in Sec. III, a self-consistent theory is developed and some expressions of the susceptibility are derived. Next, in Sec. IV, simulation results are presented and compared with theory. Section V concludes this paper with a summary and discussion.

II. MODEL AND SUSCEPTIBILITY

The model used here [10] is of the following form:

$$\frac{d\theta_j}{dt} = \Omega_j + \frac{K}{N} \sum_{k=1}^{N} s_k s_j \sin(\theta_k - \theta_j) \quad (j = 1, \ldots, N), \quad (2)$$

where Ω_j is the intrinsic frequency of the jth oscillator, $K \geqslant 0$ is the coupling strength, and s_j is the coupling parameter of the jth unit; the frequencies are set so that their distribution density within the population becomes $f(\Omega)$ in the limit $N \to \infty$; and the coupling parameters independently obey a common distribution, whose density is denoted by $P(s)$ hereafter. Note that the above model reduces to the Kuramoto model for $P(s) = \delta(s - 1)$, where $\delta(\cdot)$ is the Dirac δ function. System (2) may be the first model of randomly coupled oscillators, and nowadays there exist several analytically tractable models for large populations of randomly coupled phase oscillators [12–16]. Below we suppose that $f(\Omega)$ becomes maximum at the origin, without loss of generality, being symmetric on its both sides,

i.e., $f(-\Omega) = f(\Omega)$, and also monotonically decreasing in the region $\Omega > 0$.

We now define susceptibility χ. The phase reduction method (see Ref. [2], and references therein) tells us that a weak periodic forcing acting uniformly on all oscillators adds a term of the form $F(\omega t - \theta_j)$ to the right-hand side of Eq. (2), where F is 2π periodic and ω is the frequency of the periodic force. For simplicity, we choose a sinusoidal form as $F(\theta) = a \sin \theta$ with $a \geqslant 0$ and consider the behavior of the forced system

$$\frac{d\varphi_j}{dt} = \Delta_j + \frac{K}{N} \sum_{k=1}^{N} s_k s_j \sin(\varphi_k - \varphi_j) - a \sin \varphi_j$$
$$(j = 1, \dots, N), \tag{3}$$

where $\varphi_j \equiv \theta_j - \omega t$ and $\Delta_j \equiv \Omega_j - \omega$. Again, for simplicity, we here restrict ourselves to the case of resonant forcing, i.e., $\omega = 0$. The susceptibility χ is then defined by

$$\chi = \left(\frac{d|Z|}{da} \right)_{a=0}, \tag{4}$$

where Z is the asymptotic value for $t \to \infty$ in the infinite system ($N = \infty$). This definition is based on the observation that $|Z|$, which is a genuine measure of phase coherence, corresponds to the magnitude of the magnetization in magnetic systems [17].

III. THEORY

From now on, we set

$$Z = \frac{1}{N} \sum_{j=1}^{N} e^{i\varphi_j}, \tag{5}$$

since $|Z|$ remains the same as in its original definition, Eq. (1). We also employ another order parameter introduced in Ref. [10]:

$$D \equiv \frac{1}{N} \sum_{j=1}^{N} s_j e^{i\varphi_j}. \tag{6}$$

Then, what is done below is to set up a self-consistent equation of D and to express Z using D, as formulated in Ref. [10] for the case of no forcing ($a = 0$). The analysis made below is for the continuum limit $N \to \infty$.

Let us first note that a one-body equation of φ_j follows from Eq. (3) for each j:

$$\frac{d\varphi_j}{dt} = \Delta_j + \text{Im}\{(KDs_j + a)e^{-i\varphi_j}\}. \tag{7}$$

Then, assuming that both Z and D become asymptotically stationary, we can obtain the following results: For oscillators with $|\Delta_j| < A_j \equiv |KDs_j + a|$,

$$e^{i\varphi_j} \to e^{i\alpha_j} \left\{ \sqrt{1 - \frac{\Delta_j^2}{A_j^2}} + i\frac{\Delta_j}{A_j} \right\} \tag{8}$$

for $t \to \infty$, whereas for oscillators with $|\Delta_j| > A_j$,

$$\langle e^{i\varphi_j} \rangle = \text{sign}(\Delta_j) i e^{i\alpha_j} \left(\frac{|\Delta_j|}{A_j} - \sqrt{\frac{\Delta_j^2}{A_j^2} - 1} \right), \tag{9}$$

where $\alpha_j \equiv \text{Arg}(KDs_j + a)$ and the bracket $\langle \cdot \rangle$ stands for time average. These results may be used to find a self-consistent equation of the order parameter D, which reads

$$D = \frac{1}{N} \sum_{j=1}^{N} s_j \langle e^{i\varphi_j} \rangle$$
$$= \int_{-\infty}^{\infty} ds\, P(s)s(KDs + a)G(KDs + a), \tag{10}$$

where

$$G(z) \equiv \int_{-1}^{1} dx f(|z|x)\sqrt{1 - x^2}.$$

Use of $D_r \equiv \text{Re}D$ and $D_i \equiv \text{Im}D$ makes the last equation more explicit:

$$D_r = \int_{-\infty}^{\infty} ds\, P(s)s(KD_r s + a)G(KDs + a), \tag{11}$$

$$D_i = KD_i \int_{-\infty}^{\infty} ds\, P(s)s^2 G(KDs + a). \tag{12}$$

The order parameter Z is then given by

$$Z = \frac{1}{N} \sum_{j=1}^{N} \langle e^{i\varphi_j} \rangle$$
$$= \int_{-\infty}^{\infty} ds\, P(s)(KDs + a)G(KDs + a), \tag{13}$$

where it has been used that the only difference of Z from D is the absence of the factor s_j in its definition, Eq. (5).

For later convenience, we set up the equation of $D_0 \equiv D|_{a=0}$ using Eq. (10) [10]:

$$D_0 = KD_0 \int_{-\infty}^{\infty} ds\, P(s)s^2 G(KD_0 s). \tag{14}$$

We define K_c as the value of K at which a nontrivial solution starts to exist in the last equation, which is given by

$$K_c = \frac{2}{\pi \langle\langle s^2 \rangle\rangle f(0)}, \tag{15}$$

where the double brackets $\langle\langle \cdot \rangle\rangle$ mean an average with respect to $P(s)$. A state of the system with $Z = 0$ and $D \neq 0$ in the absence of periodic forcing was discovered and called a *spurious glass* state in Ref. [10].

A. The Kuramoto model

Let us first examine the case $P(s) = \delta(s - 1)$, in which case Eq. (3) can be thought of as a periodically forced Kuramoto model as investigated by many researchers (see, e.g., Refs. [18–21]). Taking into account that D is identical to Z in this case, we find equations of $Z_r \equiv \text{Re}Z$ and $Z_i \equiv \text{Im}Z$ either from Eqs. (11) and (12) or Eq. (13). The synchronizing nature of the external force as well as the system's reflection symmetry enable us to set $Z_i = 0$ with $Z_r \geqslant 0$ and obtain

$$Z_r = (KZ_r + a)G(KZ_r + a). \tag{16}$$

Let R denote Z_r for $a = 0$. The above equation leads to $R = KRG(KR)$, from which follows that $R = 0(K < K_c)$ and

$$1 = KG(KR) \quad (K > K_c), \tag{17}$$

where

$$K_c \equiv \frac{1}{G(0)} = \frac{2}{\pi f(0)} \tag{18}$$

is the critical coupling strength at which the transition to macroscopic synchronization occurs [2]. Looking back at Eq. (16) and differentiating its both sides by a, we obtain

$$\left(\frac{dZ_r}{da} \right)_{a=0} = \frac{\tilde{G}(R)}{1 - K\tilde{G}(R)}, \tag{19}$$

where $\tilde{G}(R) \equiv G(KR) + KRG'(KR)$ with the prime standing for differentiation. Using this result, we arrive at the formulas of the susceptibility as follows:

$$\chi = \frac{1}{K_c - K} \quad (K < K_c), \tag{20}$$

$$= -\frac{1}{K} \left\{ 1 + \frac{1}{K^2 RG'(KR)} \right\} \quad (K > K_c). \tag{21}$$

Note that the susceptibility χ follows the inverse power law throughout the subcritical region. The problem is how it behaves as K approaches K_c on the supercritical side. For this purpose, we suppose that

$$f(\Omega) = f(0) - C|\Omega|^p + \cdots \tag{22}$$

near $\Omega = 0$, where both C and p are positive constants. Then, Eq. (17) as well as Eq. (21) yield

$$\chi \simeq \frac{1}{p(K - K_c)} \tag{23}$$

for K close to K_c. It thus turns out that χ also obeys the same critical power law as it does on the subcritical side, but the critical amplitude is $1/p$ instead of unity. These scaling behaviors of the susceptibility are exactly the same as those predicted by mean-field theory in statistical mechanics [7].

For a Lorentzian distribution of natural frequencies given by

$$f(\Omega) = \frac{\gamma}{\pi} \frac{1}{\Omega^2 + \gamma^2}, \tag{24}$$

for which K_c is 2γ by Eq. (18), it is possible to get explicit expressions of χ. On the subcritical side, owing to Eq. (20), we have

$$\chi = \frac{1}{2\gamma - K} \quad (0 < K < K_c), \tag{25}$$

while on the supercritical side, noting that

$$G(r) = \frac{1}{\sqrt{r^2 + \gamma^2} + \gamma}, \tag{26}$$

we obtain

$$\chi = \frac{\gamma}{K(K - 2\gamma)} = \frac{K_c}{2K(K - K_c)} \quad (K > K_c), \tag{27}$$

in accordance with the predicted critical behavior, Eq. (23), because $p = 2$ for $f(\Omega)$ displayed in Eq. (24). For the

distribution (24), the Ott-Antonsen ansatz [22,23] is available and the above results straightforwardly come out from the evolution equation of Z derived based on the ansatz.

At this point, it is worthwhile to see if Widom's equality holds, which states that in magnetic phase transitions, there is a relation among three of critical exponents as follows [7]:

$$\gamma = \beta(\delta - 1), \tag{28}$$

where the exponents γ, β, and δ are defined as $M \propto (T_c - T)^\beta (T < T_c), \chi \propto |T - T_c|^{-\gamma}$ near $T = T_c$ and $M \propto H^{1/\delta}$ for H small at $T = T_c$, in which M is the magnetization, T_c is the critical temperature, and H denotes the intensity of the applied magnetic field. Note that γ here differs from the one in Eq. (24). The counterparts of these critical scaling laws in the present case follow from the fact that the width of $f(\Omega)$ plays the same role as the temperature, because it is the cause of desynchronization just as the temperature promotes decoherence. However, when the width is fixed and the coupling strength K is varied as supposed in this paper, the effective width is proportional to $1/K$; therefore, the above scaling laws translate into $|Z| \propto (K - K_c)^\beta \ (K > K_c), \chi \propto |K - K_c|^{-\gamma}$ near $K = K_c$, and $|Z|_{K=K_c} \propto a^{1/\delta}$ for small a. Since $\beta = 1/2$ [2] and $\gamma = 1$, what remains to be calculated is the exponent δ. By setting $K = K_c$ in Eq. (16) and expanding its right-hand side in a, we obtain

$$Z_r \cong \frac{1}{K_c(AK_c)^{1/3}} a^{1/3} \tag{29}$$

for $a \to 0$ with $A \equiv -\pi f''(0)/16$, which implies that $\delta = 3$. It has been thus confirmed that the equality (28) is valid in the present case as well. In deriving the last equation, $p = 2$ [see Eq. (22)] has been implicitly assumed. However, without this restriction, one can show quite easily that $\beta = 1/p$ and also that $\delta = p + 1$. Widom's equality is therefore not violated for any $p > 0$.

B. The most random coupling

Here we are concerned with the case of $P(-s) = P(s)$, so that the average value of every coupling parameter is zero. This case is discussed in Ref. [10] in the absence of the periodic perturbation ($a = 0$). On the basis of empirical observations (see Sec. IV) and the analysis performed in the next subsection for the Mattis coupling, we assume that $D_i = \text{Im}D \neq 0$. Then, Eq. (12) gives

$$1 = K \int_{-\infty}^{\infty} ds\, P(s) s^2 G(KDs + a). \tag{30}$$

Besides this, by substituting the above equation into Eq. (11), we obtain

$$0 = \int_{-\infty}^{\infty} ds\, P(s) s\, G(KDs + a) \quad (a > 0). \tag{31}$$

Now, paying attention to Eq. (13) and using the last equation, we find a simplified expression of Z as follows:

$$Z = a \int_{-\infty}^{\infty} ds\, P(s) G(KDs + a), \tag{32}$$

which implies $\mathrm{Im}Z = 0$. The susceptibility is thus given by

$$\chi = \int_{-\infty}^{\infty} ds\, P(s) G(KD_0 s). \tag{33}$$

As long as the system's state with $D_i \neq 0$ is stable at least for small a, Eqs. (30)–(33) hold irrespective of $P(s)$; in fact, its symmetry $P(-s) = P(s)$ has not been invoked above.

The assumed symmetry of $P(s)$ may be used to obtain the value of D_r. Note that

$$|KDs + a| = \sqrt{(KD_r s + a)^2 + (KD_i s)^2}.$$

Hence, if $D_r = 0$, then Eq. (31) automatically holds, since the integrand becomes an odd function of s in that case. This result is supported by numerical results presented in Sec. IV as well as the stability analysis done in Subsec. III C for a particular case of $P(s)$ with the same symmetry as supposed here.

Let us now consider the behavior of χ given in Eq. (33). For $a = 0$, as demonstrated in Ref. [10], $D_0 = 0$ for $K \leqslant K_c$ and $D_0 \neq 0$ otherwise, while Z is always zero due to Eq. (32). What happens at $K = K_c$ is therefore a transition to the spurious glass phase, as referred to earlier. According to Eq. (33), we conclude that

$$\chi = G(0) = \frac{1}{\langle\langle s^2 \rangle\rangle K_c} \tag{34}$$

in the range $0 \leqslant K \leqslant K_c$ and moreover that χ decreases as K grows in the supercritical region, which is because $f(\Omega)$ monotonically decreases for increasing $|\Omega|$, as assumed previously. To sum up, at the transition to the spurious glass phase, the susceptibility does not diverge, but instead exhibits a cusp. Furthermore, it remains constant in the subcritical region. These results are in remarkable contrast with the behavior of χ in the case of the Kuramoto model.

A remark is now in order. According to Eq. (30), the boundary in the (K, a) phase diagram where a nontrivial solution to it begins to appear is given by

$$K = \frac{1}{\langle\langle s^2 \rangle\rangle G(a)}. \tag{35}$$

C. The Mattis coupling

Here we discuss the dynamics of the two order parameters for the case of

$$P(s) = \tfrac{1}{2}\{\delta(s - 1) + \delta(s + 1)\}, \tag{36}$$

i.e., s_j taking ± 1 alone with equal probabilities. This coupling was first introduced in a theoretical study of spin glasses [24] and then studied for the first time in the context of coupled oscillators [10]. This coupling would be the simplest example of the symmetric $P(s)$ discussed in the previous subsection. Here we confine ourselves to Lorentzian distributions of intrinsic frequencies, as shown in Eq. (24), to employ the Ott-Antonsen approach. The purpose here is to support the assumption made in the previous subsection about the stability of the states with $D_r = 0$ and $D_i \neq 0$ in the supercritical region in the presence of the periodic force.

Let $p(\varphi, t, \Omega, s)$ be the phase distribution density at the intrinsic frequency Ω and the coupling parameter s and introduce

$$\alpha(t, \Omega, s) \equiv \int_0^{2\pi} p(\varphi, t, \Omega, s) e^{i\varphi} d\varphi. \tag{37}$$

The Ott-Antonsen ansatz [22,23] then yields the evolution equations of α's by way of Eq. (7):

$$\frac{d\alpha}{dt} = i\Omega\alpha - \frac{\alpha^2}{2}(KsD^* + a) + \frac{1}{2}(KsD + a), \tag{38}$$

in which the asterisk stands for complex conjugate. It is also possible to obtain the following expressions of the two order parameters (see Ref. [15] for a similar analysis for a different model):

$$Z = \tfrac{1}{2}\{\alpha(t, i\gamma, 1) + \alpha(t, i\gamma, -1)\}, \tag{39}$$

$$D = \tfrac{1}{2}\{\alpha(t, i\gamma, 1) - \alpha(t, i\gamma, -1)\}. \tag{40}$$

Using the equations of $\alpha(t, i\gamma, \pm 1)$ found from Eq. (38) and the above expressions, we can obtain the evolution equations of Z and D as follows:

$$\frac{dZ}{dt} = -\gamma Z - K|D|^2 Z + \frac{a}{2}(1 - Z^2 - D^2), \tag{41}$$

$$\frac{dD}{dt} = \left(-\gamma + \frac{K}{2}\right)D - \frac{K}{2}(Z^2 + D^2)D^* - aZD. \tag{42}$$

For convenience, we transform these equations into those of x, y, z and w, where $Z = x + iy$ and $D = z + iw$ with all the new variables real, to obtain

$$\frac{dx}{dt} = -\gamma x - K(z^2 + w^2)x + \frac{a}{2}(1 - x^2 + y^2 - z^2 + w^2), \tag{43}$$

$$\frac{dy}{dt} = -\gamma y - K(z^2 + w^2)y - a(xy + zw), \tag{44}$$

$$\frac{dz}{dt} = \left(-\gamma + \frac{K}{2}\right)z - \frac{K}{2}\{(x^2 - y^2 + z^2 + w^2)z + 2xyw\} - a(xz - yw), \tag{45}$$

$$\frac{dw}{dt} = \left(-\gamma + \frac{K}{2}\right)w - \frac{K}{2}\{(-x^2 + y^2 + z^2 + w^2)w + 2xyz\} - a(xw + yz). \tag{46}$$

First of all, we focus on those fixed points of the above equations at which $y = z = w = 0$, implying that the order parameter D vanishes there; the remaining coordinate is given by

$$x = \frac{-\gamma \pm \sqrt{\gamma^2 + a^2}}{a} \equiv x_{\pm}. \tag{47}$$

A linear stability analysis indicates that the fixed point with $x = x_-$ is always unstable while the other with $x = x_+$, referred to as fixed point A, is stable in the regions $a \geqslant 0$ ($K < 2\gamma$) and $a > \sqrt{K(K - 2\gamma)}$ ($K > 2\gamma$) (see Fig. 1). This boundary is consistent with Eq. (35).
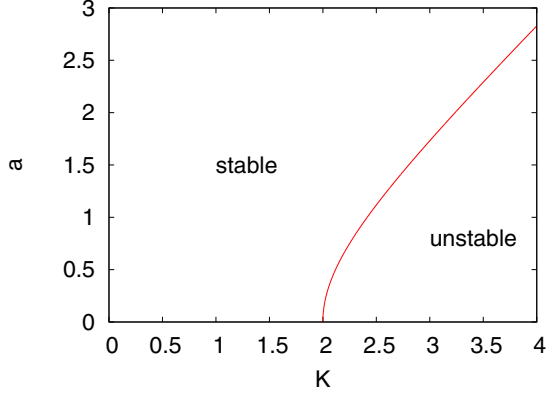
FIG. 1. (Color online) The stability boundary of fixed point A for $\gamma = 1$, where the boundary is given by $a = \sqrt{K(K - 2\gamma)}$ $(K > 2\gamma)$ (see text).

Let us now treat fixed points with $y = z = 0$, i.e., those representing the state of $\mathrm{Re}\, D = 0$, for which we have the following equations of x and w:

$$x^3 - \frac{2a}{K}x^2 + \left(1 - \frac{\gamma}{K} + \frac{a^2}{K^2}\right)x - \frac{1}{K}\left(1 - \frac{\gamma}{K}\right)a = 0, \quad (48)$$

$$w^2 = x^2 - \frac{2a}{K}x + 1 - \frac{2\gamma}{K}. \quad (49)$$

It can be shown that fixed points of this type are limited to the following two:

$$x = \frac{a}{K}, \quad w = \pm\sqrt{1 - \frac{2\gamma}{K} - \frac{a^2}{K^2}}, \quad (50)$$

which exist in the region where the fixed point A is unstable, i.e., $0 \leqslant a < \sqrt{K(K - 2\gamma)}$ $(K > 2\gamma)$ (see Fig. 1). Hereafter, the one with $w > 0$ and the other with $w < 0$ are denoted by B_+ and B_-, respectively. The Jacobians of the dynamical system (43)–(46) at these fixed points can be shown to have all eigenvalues in common, which are

$$\gamma - K, \quad \gamma - K, \quad -\frac{a^2}{K}, \quad 2\gamma - K + \frac{a^2}{K},$$

revealing that the fixed points $B_\pm$ are stable in their existing region. By looking back at Fig. 1, it is also evident that a supercritical pitchfork bifurcation takes place on the stability boundary of the fixed point A, where A and $B_\pm$ collide.

Finally, we examine the stability of fixed points with $y = w = 0$ corresponding to $\mathrm{Im}\, D = 0$. In this case, x and z obey

$$x^3 + \frac{2a}{K}x^2 + \left(-1 + \frac{\gamma}{K} + \frac{a^2}{K^2}\right)x + \frac{\gamma}{K^2}a = 0, \quad (51)$$

$$z^2 = -x^2 - \frac{2a}{K}x + 1 - \frac{2\gamma}{K}. \quad (52)$$

For $a = 0$, these equations have solutions only for $K > 2\gamma$, which are

$$x = 0, \quad z = \pm\sqrt{1 - \frac{2\gamma}{K}}. \quad (53)$$

Although details are omitted, it can be shown perturbatively that the largest stability eigenvalue λ for each fixed point of

the present type is given by

$$\lambda = \frac{a^2}{K} + \text{higher order in } a \quad (54)$$

for a small, so that this type of fixed point is irrelevant to the purpose of evaluating χ, since it is unstable in the limit $a \to 0$.

Finally, noting $Z = x$, we can obtain expressions of the susceptibility χ from the stable fixed points, namely, A in the subcritical region and $B_\pm$ in the supercritical region:

$$\chi = \frac{1}{2\gamma} \quad (0 < K \leqslant 2\gamma), \quad (55)$$

$$= \frac{1}{K} \quad (K > 2\gamma). \quad (56)$$

These results are in exact agreement with those predicted from the formula (33). To be more specific, substituting the form of $P(s)$ into Eq. (33), we find that $\chi = G(K D_0)$. Note also that Eq. (15) gives $K_c = 2\gamma$. Hence, Eq. (55) agrees with Eq. (34),

FIG. 2. (Color online) The susceptibility χ for the Kuramoto model with a Lorentzian distribution of natural frequencies with $\gamma = 1$. Note that $K_c = 2$ here. The symbols (red +, green ×, blue asterisk, purple square) are simulation results for $N = 10\,000$, while the curves are due to theory. The numbers in the legend show the values of a.
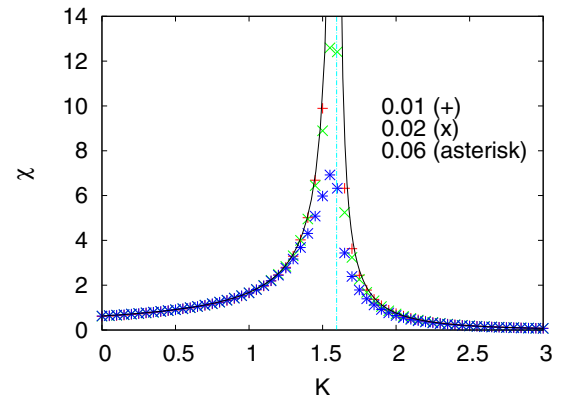
FIG. 3. (Color online) The susceptibility χ for the Kuramoto model with a Gaussian distribution of natural frequencies whose standard deviation is one. The vertical broken line locates the threshold K_c. Other details are the same as in Fig. 2.
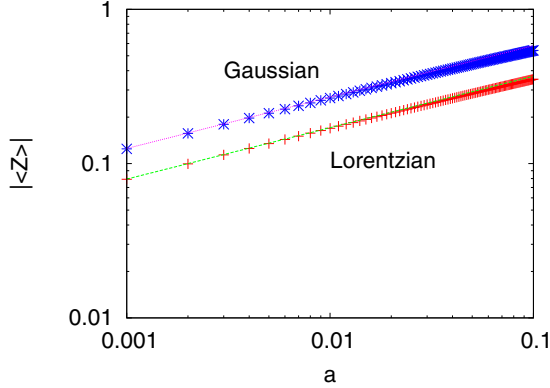
FIG. 4. (Color online) The behavior of R at the critical point $K = K_c$ in the Kuramoto model. The straight lines show the right-hand side of Eq. (29) for a Lorentzian distribution ($\gamma = 1$) and a Gaussian distribution (variance = 1). The time step is 0.01.

since $\langle\langle s^2 \rangle\rangle = 1$. For $K > K_c$, again using the form of $P(s)$ in Eq. (14), we realize that $\chi = G(K D_0) = 1/K$, in harmony with Eq. (56).

The simple example of the most random case studied above indicates that the states with $D_r = 0$ and $D_i \neq 0$, which correspond to fixed points $B_\pm$, are stable, while the states with $D_r \neq 0$ and $D_i = 0$ are unstable at least for small a. This supports the analysis of the most random case performed earlier.

IV. NUMERICAL RESULTS

This section is devoted to numerical verification of the theory developed in the preceding section. Numerical simulations were performed with the fourth-order Runge-Kutta method with the time step 0.05 unless stated otherwise. Initial values of the phase variables φ_j were taken randomly in the interval $[0, 2\pi]$. In each run, the first part of computation, typically $0 \leqslant t \leqslant 1000$, was discarded as a transient period. In order to diminish finite-size effects, the susceptibility χ was calculated using the time-average of Z as $\chi = |\langle Z \rangle|/a$; however, for the nonrandom case with $K > K_c$, χ was

evaluated as $(|\langle Z \rangle| - |\langle Z \rangle|_{a=0})/a$; in each case, a was set to be small (see figures for details). Intrinsic frequencies were set without using a random number generator [25], while the coupling parameters s_j in the random case were produced by subroutines from IMSL.

Figures 2 and 3 display the behavior of χ in the case of the Kuramoto model $[P(s) = \delta(s - 1)]$ for $f(\Omega)$ Lorentzian with $\gamma = 1$ and Gaussian with standard deviation $\sigma = 1$, respectively. The curves are theoretical results; those on the subcritical side are based on Eq. (20), whereas those on the supercritical side are drawn using Eq. (27) in Fig. 2 and Eq. (21) as well as numerical solutions to Eq. (17) in Fig. 3. Simulation results are presented for some values of a. In each figure, agreement with theory is seen to improve as a decreases toward zero as it should be, especially in the critical region. Figure 4 gives evidence for $\delta = 3$ as derived at the end of Subsec. III A, where nice agreement is found between the theoretical and the simulation results as K approaches K_c.

Next, in Fig. 5, the behavior of the susceptibility is shown for the Mattis coupling with $f(\Omega)$ Lorentzian of $\gamma = 1$ and $P(s)$ as displayed in Eq. (36). The theoretical results presented there are due to Eqs. (55) and (56). Each simulation result in Fig. 5(a) is an average over 100 realizations of the coupling parameters. Moreover, Fig. 5(b) indicates how χ varies with K for all the realizations used in Fig. 5(a). Although the sample dependence is much larger in the supercritical region, the averaged values of χ are in excellent agreement with theory. In particular, the remarkable cusp singularity at the critical point should be noticed.

Let us now investigate the case in which both $f(\Omega)$ and $P(s)$ are the same Gaussian distributions with average 0 and standard deviation $\sigma = 1$. Figure 6(a) presents a phase diagram with the boundary between the regions $D = 0$ and $D \neq 0$ drawn using Eq. (35). It should be noticed that this phase diagram is quite similar to the one in Fig. 1. The behavior of $|D|$ is examined in Fig. 6(b), where numerical solutions to Eq. (30) are in excellent agreement with the simulation results.

We now check the dynamic behavior of D before proceeding to the examination of χ. Actually, numerical simulation reveals that a finite-size effect is so strong that the argument of D, denoted by ψ, continues to drift even for $N = 200\,000$,
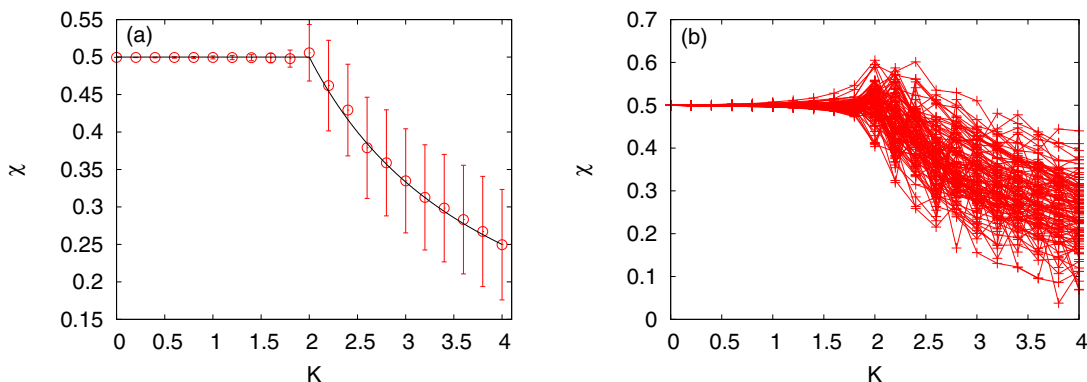
FIG. 5. (Color online) The susceptibility for the case of the Mattis coupling, where $N = 20\,000, a = 0.05$, and $f(\Omega)$ is a Lorentzian with $\gamma = 1$. (a) $|\langle Z \rangle|/a$ averaged over 100 realizations of the coupling parameters $\{s_j\}$ (red circle). The length of each error bar is double the standard deviation. The lines are theoretical results. (b) The behavior of the same quantity for all the realizations used in panel (a), where all data from each realization are connected by line segments.
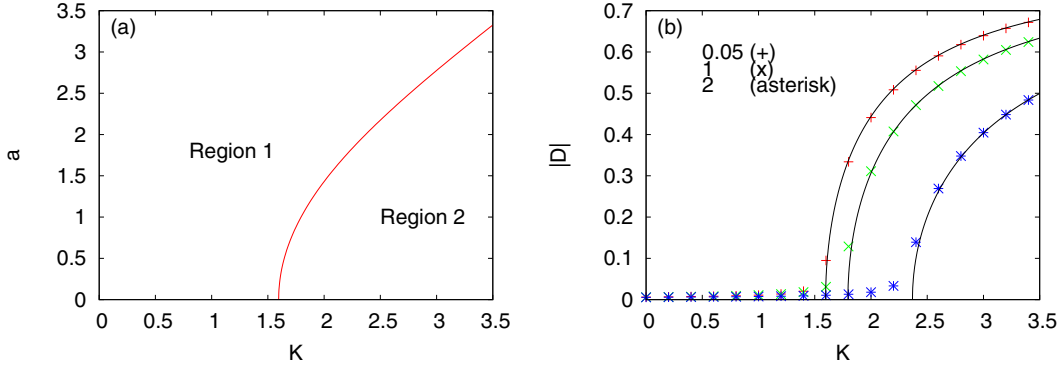
FIG. 6. (Color online) The behavior of the order parameter D when both $f(\Omega)$ and $P(s)$ are the same Gaussian distributions with the standard deviation of one. (a) The boundary between the region where only the solution $D = 0$ exists (region 1) and the one where nontrivial solutions $D_r = 0, D_i \neq 0$ add to it (region 2). (b) Comparison between theory and simulation concerning $|D|$. The symbols (red +, green ×, blue asterisk) show the time averages of $|D|$ averaged over 100 realizations of the coupling parameters $\{s_j\}$ for $N = 20\,000$. The curves are based on theory. The numbers in the legend give the values of a.

provided the magnitude of forcing a is small enough. This finding is reported in the form of the distribution of ψ in Fig. 7, which shows the results for $N = 2000$ and $200\,000$. The argument ψ is expected to eventually settle at either $\pi/2(D_r = 0, D_i > 0)$ or $3\pi/2(D_r = 0, D_i < 0)$. In both panels of Fig. 7, it is seen that this is the case only when a is not very small. The fact that consistency with theory is better for larger N indicates that the drift of ψ is a finite-size effect. Hence, if a is small, then the finite-size effect outcompetes the synchronizing effect of the periodic force, causing ψ to be nonstationary; if a is sufficiently large, the opposite is the case and hence ψ becomes asymptotically stationary, as clearly observed in Fig. 7.

Figure 7(b) shows that the distribution of $\psi/(2\pi)$ for $a = 0.3$ has a single peak at the bin centered at $1/4$ for each of the two different realizations of the coupling parameters. For $a = 0.2$, this is not the case, but the distributions are fairly close to those for $a = 0.3$ (data not shown). On the basis of these observations, the susceptibility has been computed for $a = 0.25$ with $N = 200\,000$ and the results are displayed in Fig. 8. The agreement with theory found in Fig. 8(a) is not as good as in other cases, but seems satisfactory, considering that a is much more away from zero. Figure 8(b) shows a collection of χ's behaviors for all realizations of $\{s_j\}$ used to obtain χ in Fig. 8(a). The sample dependence observed here

seems weaker than in Fig. 5(b), which would stem from the far larger system size adopted here.

V. SUMMARY AND DISCUSSION

The concept of susceptibility χ has been introduced for populations of coupled oscillators and its behavior has been elucidated numerically as well as analytically for large ensembles of phase oscillators with the coupling $Ks_i s_j/N$ between oscillators i and j proposed in Ref. [10], which includes the uniform all-to-all coupling and the Mattis coupling as particular cases. A general theory has been developed for the two order parameters Z and D under a resonant periodic forcing, which may be used not only to study χ's behavior but also to investigate the response of the system to periodic perturbation with an arbitrary amplitude. This theory predicts a remarkable difference in the behavior of the susceptibility between the nonrandom case (the Kuramoto model), in which all s_j are the same, and the most random case, in which s_j are distributed symmetrically about the origin. Namely, in the former case, χ diverges at the critical coupling strength as it is approached from its both sides obeying the scaling $|K - K_c|^{-1}$, which is known as a conventional behavior of mean-field models in statistical physics [7]. It has
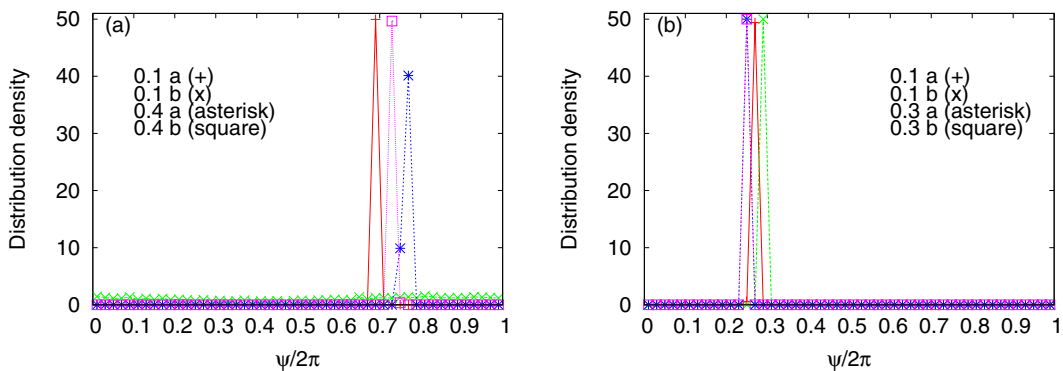
FIG. 7. (Color online) Distribution densities of $\psi \equiv \text{Arg}D$ in the range $1000 < t < 21\,000$ for the same $f(\Omega)$ and $P(s)$ as in Fig. 6. The densities were computed by dividing the interval $[0, 2\pi]$ into 50 bins (red +, green ×, blue asterisk, purple square). Each number in the legends show a's value, while "a" and "b" therein indicate different realizations of $\{s_j\}$. (a) $N = 2000$. (b) $N = 200\,000$.
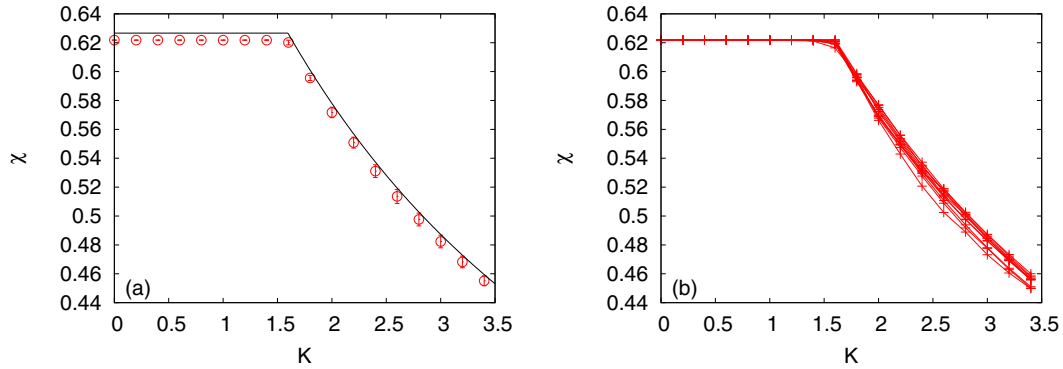
FIG. 8. (Color online) The susceptibility χ for the same $f(\Omega)$ and $P(s)$ as in Figs. 6 and 7. (a) The symbols are simulation results for $N = 200\,000$ and $a = 0.25$, showing $|\langle Z \rangle|/a$ averaged over 10 realizations of the coupling parameters (red circle). The lines are theoretical results. (b) The behavior of $|\langle Z \rangle|/a$ for all the realizations used in panel (a). Other details are the same as in Fig. 5.

been demonstrated that the Widom equality $\gamma = \beta(\delta - 1)$ is satisfied in the present case as well. By contrast, in the latter case, χ remains constant until the system enters the spurious glass phase, where the susceptibility decreases as K grows. In this case, a cusp is formed at the critical point. In fact, it is known that the magnetic susceptibility exhibits a cusp at the critical temperature in the Mattis model of spin glasses, but it does not keep a constant value in the subcritical region, unlike our corresponding model [26].

A possible reason for the susceptibility to be finite at the critical point in the most random case is that Z remains zero even after the system enters the spurious glass phase, implying that its zero value is "stable." On the other hand, in the case of the uniform coupling (the Kuramoto model), it becomes neutrally stable at $K = K_c$, thereby causing the divergence of χ as the critical point is approached. The reason why χ does not vary in the subcritical region may be explained intuitively in the following way: The dynamics of each oscillator is driven by D [see Eq. (7)], but the random coupling parameters involved in it keep D vanishingly small by canceling the synchronizing effect of the weak periodic force and hence χ maintains its value for $K = 0$, whereas in the Kuramoto model, each oscillator is governed by Z, which directly reflects the synchronizing effect of the external force and therefore χ increases with K.

These results may be of significance in controlling the system's behavior, especially the degree of its phase coherence, and also in foreseeing any critical phenomenon as a parameter is varied. χ's behavior also reflects the nature of coupling among constituent oscillators and therefore experimental observations of χ may be useful in identifying the type of coupling working in a population. For these reasons, it would be an interesting and crucial subject to investigate χ's behavior extensively for a variety of couplings and a number of networks, whether simple or complex.

As remaining subjects, it would be necessary to establish the stability of the states with $D_r = 0$ and $D_i \neq 0$ in the most random case for a general class of $P(s)$ that is symmetric about $s = 0$; this task has been done here only for the Mattis coupling when $f(\Omega)$ is a Lorentzian. Furthermore, the intermediate case should also be studied in which $P(s)$ is neither a δ function nor an even function. The effects of strong frustration [27] and aging [28] on χ are also interesting and important subjects. These problems are now under study and will be reported elsewhere.

[1] A. T. Winfree, *The Geometry of Biological Time* (Springer, New York, 2001).

[2] Y. Kuramoto, *Chemical Oscillations, Waves, and Turbulence* (Springer, Berlin, 1984).

[3] A. Pikovsky, M. Rosenblum, and J. Kurths, *Synchronization: A Universal Concept in Nonlinear Sciences* (Cambridge University Press, Cambridge, 2001).

[4] A. T. Winfree, J. Theor. Biol. **16**, 15 (1967).

[5] S. H. Strogatz, Nature (London) **410**, 268 (2001).

[6] J. A. Acebrón, L. L. Bonilla, C. J. P. Vicente, F. Ritort, and R. Spigler, Rev. Mod. Phys. **77**, 137 (2005).

[7] H. E. Stanley, *Introduction to Phase Transitions and Critical Phenomena* (Oxford University Press, Oxford, 1971).

[8] H. Daido, Prog. Theor. Phys. **88**, 1213 (1992).

[9] H. Daido, Phys. D (Amsterdam, Neth.) **91**, 24 (1996).

[10] H. Daido, Prog. Theor. Phys. **77**, 622 (1987).

[11] Y. Kuramoto, in *International Symposium on Mathematical Problems in Theoretical Physics*, edited by H. Araki, Lecture Notes in Physics No. 39 (Springer, New York, 1975).

[12] L. Bonilla, C. P. Vicente, and J. Rubi, J. Stat. Phys. **70**, 921 (1993).

[13] H. Hong and S. H. Strogatz, Phys. Rev. Lett. **106**, 054102 (2011).

[14] H. Hong and S. H. Strogatz, Phys. Rev. E **85**, 056210 (2012).

[15] I. M. Kloumann, I. M. Lizarraga, and S. H. Strogatz, Phys. Rev. E **89**, 012904 (2014).

[16] D. Iatsenko, P. V. E. McClintock, and A. Stefanovska, Nat. Commun. **5**, 4118 (2014).

[17] A similar susceptibility is studied for a Hamiltonian mean-field system in S. Ogawa, A. Patelli, and Y. Y. Yamaguchi, Phys. Rev. E **89**, 032131 (2014); S. Ogawa and Y. Y. Yamaguchi, *ibid.* **89**, 052114 (2014). Note, however, that the physical context of these studies is quite different from ours: The former is about a conservative system as a model of an XY-spin system, while the latter about dissipative systems as models of large-scale coupled limit-cycle oscillators.

[18] H. Sakaguchi, Prog. Theor. Phys. **79**, 39 (1988).

[19] T. M. Antonsen, R. T. Faghih, E. Ott, and J. Platig, Chaos **18**, 037112 (2008).

[20] L. M. Childs and S. H. Strogatz, Chaos **18**, 043128 (2008).

[21] L. F. Lafuerza, P. Colet, and R. Toral, Phys. Rev. Lett. **105**, 084101 (2010).

[22] E. Ott and T. M. Antonsen, Chaos **18**, 037113 (2008).

[23] E. Ott and T. M. Antonsen, Chaos **19**, 023117 (2009).

[24] D. C. Mattis, Phys. Lett. A **56**, 421 (1976).

[25] Intrinsic frequencies are set in the following way: For the distribution (24) with $\gamma = 1$, $\Omega_j = \tan\{(\pi/N)j - (N+1)\pi/(2N)\}$ and for the Gaussian distribution $f(\Omega)$ with average $= 0$ and variance $= 1$, $\Omega_j = (x_{j-(N/2)-1} + x_{j-(N/2)})/2$ for $j = (N/2) + 1, \ldots, N$ and $\Omega_j = -\Omega_{N+1-j}$ for $j = 1, \ldots, N/2$, where x_k are recursively defined as $1/N = (x_{k+1} - x_k)f(x_k)$ with $x_0 = 0$.

[26] R. Bidaux, J. P. Carton, and G. Sarma, Phys. Lett. A **58**, 467 (1976).

[27] H. Daido, Phys. Rev. Lett. **68**, 1073 (1992).

[28] H. Daido and K. Nakanishi, Phys. Rev. Lett. **93**, 104101 (2004).